Dynamic light scattering study of the non-exponential α-relaxation in sodium germanate glass melts

D. L. Sidebottom

Creighton University

Abstract

Photon correlation spectroscopy is used to measure the dynamic structure factor in a series of network-forming sodium germanate glass melts at temperatures near but above the glass transition. In addition to the primary α-relaxation, a slower diffusive process is identified with the diffusion of mobile Na cations within the oxide network. Along with determination of the glass transition temperature and fragility index, the non-exponentiality of the α-relaxation is characterized and compared with previous studies in sodium phosphate and sodium borate melts. A key result found here is a temperature-dependent stretching exponent which uniformly approaches a universal value of β = 0.5 in all three oxide systems as the glass transition is approached.

1. Introduction

An intriguing feature of super cooled liquids is the development of highly non-exponential viscoelastic relaxation as cooling proceeds close to the liquid-to-glass transition temperature, T_g, where the timescales for molecular rearrangements begin to exceed 100s of seconds[1,2]. In dynamic light scattering studies, the decay of density fluctuations that define the dynamic structure factor[3] of the liquid decay in fashion that is best described as a KWW (Kohlrausch-Williams-Watt) or stretched exponential decay of the form

$$S(q,t) = f_q exp\{-(t/\tau_\alpha)^\beta\}, \quad (1)$$

where the stretching exponent ranges from 0 < β < 1 and the average relaxation time is given as

$$\langle\tau_\alpha\rangle = \int_0^\infty exp\{-(t/\tau_\alpha)^\beta\}dt = \frac{\Gamma(1/\beta)\tau_\alpha}{\beta}. \quad (2)$$

The stretching of the decay process, which increases as the value of β decreases, is thought to characterize either the cooperativity needed for molecular rearrangements occurring in a homogeneous manner or a distribution of relaxation times, whose FWHM is approximately[4] $1.14/\beta$ decades, for a heterogeneous process wherein rearrangements occur independent of others.

In addition to the non-exponentiality, the viscoelastic relaxation - also commonly known as the α-relaxation - has a relaxation time $\tau_\alpha(T)$ that frequently deviates from simple Arrhenius temperature dependence when examined over extreme temperature ranges[1,2]. The degree of this deviation is commonly characterized by a fragility index[2],

$$m = \left.\frac{d\log_{10}\langle\tau_\alpha\rangle}{d(T_g/T)}\right|_{T\to T_g}, \quad (3)$$

which varies from m > 60 for a wide variety of molecular liquids and organic polymers[4] to m < 20 for most conventional oxide glasses (e.g., SiO_2) for which the relaxation time is most nearly Arrhenius.

Many studies of the α-relaxation have been reported over the years using either photon correlation spectroscopy or broadband dielectric spectroscopy[5,6]. The vast majority of these studies have been conducted on relatively fragile molecular liquids and organic polymers with T_g values that are often sub-ambient. By comparison, similar investigations[7,8] of network-forming oxides (NFOs, like B_2O_3 and As_2O_3) are extremely rare. In recent years, we have

endeavored to fill in this data gap by performing photon correlation spectroscopy (PCS) studies of a variety of alkali-modified NFOs including sodium phosphate[9], sodium alumina phosphate[10] and sodium borate[11] glass melts. These studies have revealed interesting trends in how the fragility of these melts is influenced by changes in the bond density of the oxide network wrought by alkali substitution and includes bond structures that range from 2d chains of connected tetrahedra to a 3d continuous random network of corner-sharing tetrahedra. Here, we report results for sodium germanate melts to demonstrate how increases in the bond density of the oxide network caused by adding alkali oxide results in an increasing fragility along with complex compositional variations in the stretching exponent. Germanate glasses possess unique optical properties including high transmission and refractive index and are often mixed with silicates to produce low phonon hosts for the incorporation of rare earth ions.[**]

2. Experimental

2.1 Sample Preparation

For $x \geq 3$ mol% Na_2O, samples of $(Na_2O)_x(GeO_2)_{100-x}$ were batched using GeO_2 (99.9999%) and Na_2CO_3 (99.98%). To eliminate insoluble specular contaminates, the sodium carbonate was further dissolved in water, passed through a 0.22 micron filter, and baked to remove water before use. Batches were melted in a Pt crucible at temperatures between 1200 to 1300 C and stirred repeatedly using a Pt rod to improve homogeneity of the melt prior to pouring into a brass mold to produce glass rods (approximately 4 mm dia. by 3 cm length) which were transparent and colorless and stored in a desiccator for later analysis. An excess of glass

produced at x = 3 mol% Na_2O was ground to a fine powder to be batched with GeO_2 to obtain powder mixtures corresponding to compositions with x = 2, 1, and 0.3 mol% Na_2O.

Light scattering samples were produced by either remelting ingots (for $x \geq 3$ mol%) or melting the powder mixture (for $x < 3$ mol%) in a 6mm ID x 8 mm OD silica ampoule which served as the light scattering cell. Samples were melted to obtain a clear, transparent liquid and were degassed (approximately 200 mTorr) before being transferred directly to a pre-heated optical oven for study.

2.2 Photon Correlation Spectroscopy

Vertically polarized laser light (532 nm) was focused to a 50 micron beam inside the sample and the intensity of light scattered at 90° (with scattering wavevector $q = \frac{4\pi n}{\lambda} \sin {}^{\theta}/_{2} = 25.05\ \mu m^{-1}$) was imaged onto a 50 micron pinhole and allowed to diffract approximately 40 cm to the photo sensitive region of a photomultiplier tube. Fluctuations in the scattered intensity driven by inherent density fluctuations in the liquid result in variations in the number of photopulses detected, $I(t')$. Photopulses are digitized and input to a commercial correlator which computes the intensity-intensity autocorrelation function (ACF):

$$C(t) = \frac{\langle I(t\prime)I(t\prime+t)\rangle}{\langle I(t\prime)\rangle^2} = 1 + A_{COH}|S(q,t)|^2, \quad (4)$$

which provides a direct representation of the dynamic structure factor associated with the decay of density fluctuations in the liquid[3]. The coherence factor, $A_{COH} = 0.80$, is an instrumental constant representing the signal-to-noise for detecting intensity variations and is calibrated separately. Autocorrelation functions were obtained at selected fixed temperatures as the melt was cooled to near T_g.

3. Results

3.1 Autocorrelation Functions

Successful samples free of crystallization and phase separation were obtained for x = 0 to 12 mol% Na_2O. Attempts to produce compositions at x ≥ 15 mol% Na_2O, were prone to crystallization when cooled slowly and could not be studied. Measurements on pure GeO_2 reported previously[12] exhibited ACFs with a single stretched relaxation whose timescale increased in a nearly Arrhenius manner with m = 16.7. However, as shown in Fig. 1, the

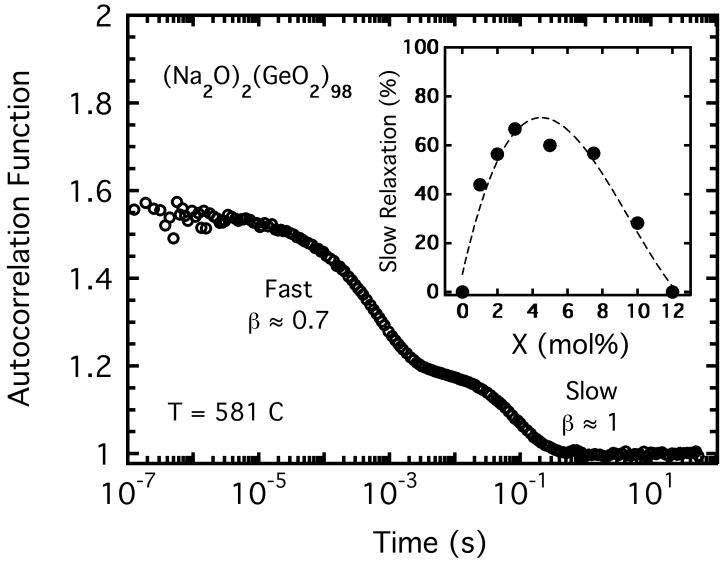

Fig. 1 Autocorrelation function measured at 581 C in x = 2 mol% Na_2O demonstrating two decay processes. Inset shows compositional dependence of relative strength of the slow relaxation.

addition of sodium oxide produces ACFs with two separated relaxation processes: a fast relaxation at short times followed by a slower relaxation at longer times. A separate investigation of the ACF collected at a series of different scattering angles confirmed that while the fast relaxation is angle independent (and thus q-independent), the slow relaxation is clearly

q^{-2}-dependent indicative of a diffusive process. Given its q-independence, stretched exponential form and approach of its decay timescale to values near 100 seconds at T_g, we can confidently assign the fast relaxation to be the viscoelastic α-relaxation of interest. As for the slow relaxation, its nearly exponential decay and q^{-2}-dependence on scattering wavevector make it very similar with the slow relaxation we observed previously[11] in sodium borate melts which we attributed to density fluctuations arising from ionic motion of the sodium ions within the oxide network. As shown in the inset to Fig. 1, the relative portion of the overall dynamic structure factor associated with this slow relaxation is zero at x = 0 mol%, increases with initial addition of Na_2O, but then vanishes again above x = 10 mol%. Whenever the slow process is present, an additional decay is included in our curve fitting of the ACF as

$$C(t) = 1 + A_{COH}\left|A_F exp\{-(t/\tau_\alpha)^\beta\} + A_S exp\{-(t/\tau_S)\}\right|^2, \quad (5)$$

where for a diffusive process, the diffusivity can be determined as $D = (\tau_S q^2)^{-1}$.

3.2 Primary α-relaxation

Curve fitting of the ACFs results in both τ_α and β from which the average relaxation time, $\langle\tau_\alpha\rangle$, can be determined (see Eq. 2). Results are plotted as a function of inverse temperature in Fig. 2 for all compositions studied and show a dramatic increase of relaxation time spanning some eight decades. The glass transition temperatures were determined by

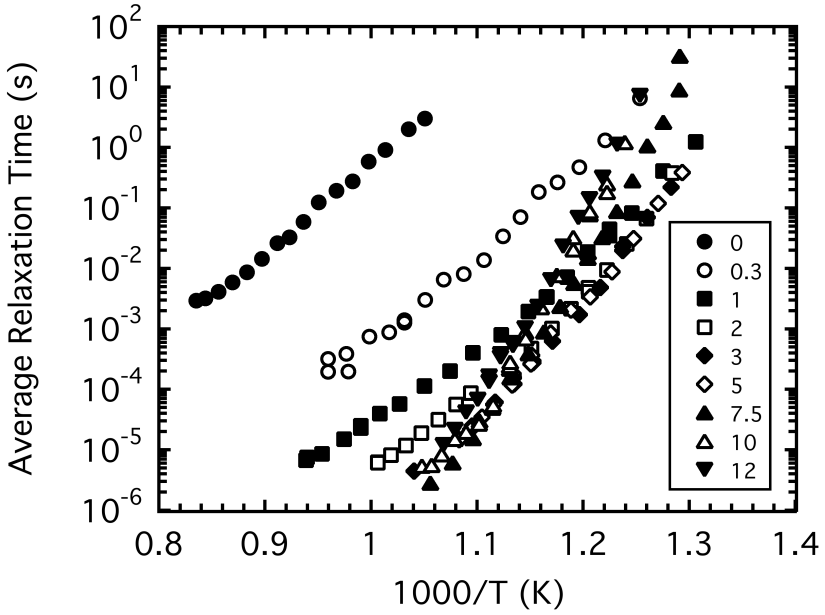

Fig. 2 Temperature dependence of the average relaxation time for the α-relaxation. Values in key are mol% Na_2O.

extrapolation of these plots to 100 seconds and the results are plotted in Fig. 3 where good agreement is seen with results from the literature obtained by viscosity studies[13,14]. The glass transition temperature of GeO_2 is found to be 585 C and drops abruptly by nearly 200 K with as little as 1 to 2 mol% Na_2O before increasing with alkali oxide.

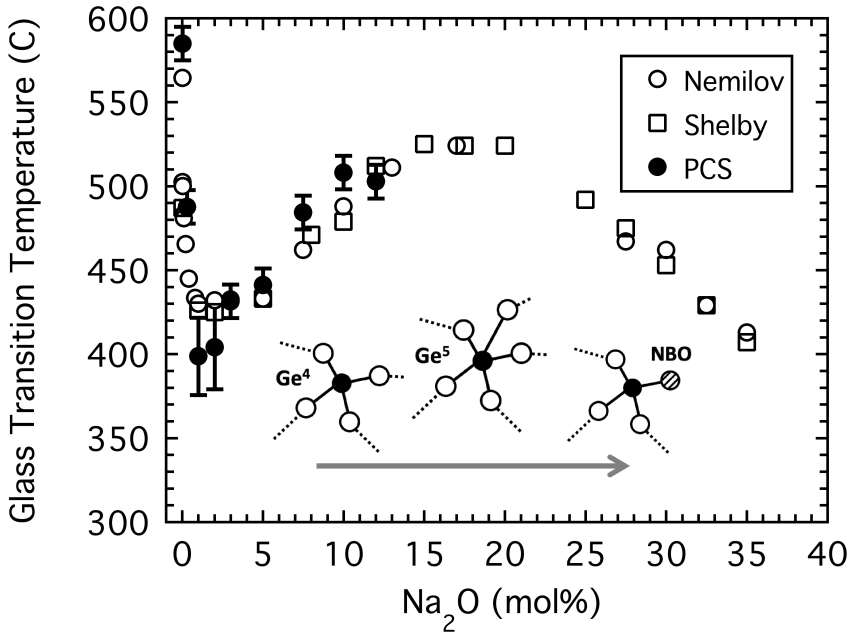

Fig. 3 Compositional variation of the glass transition temperature as determined in the present study (PCS) and from viscosity studies by Nemilov[13] and Shelby[14]. Cartoons illustrate the increase and decrease of bond connectivity associated with the germanate anomaly discussed in the text.

Having determined T_g, data like that in Fig. 2 can be plotted versus T_g/T from which the fragility index can be determined (see Eq. 3). Results provided in Fig. 4 again show good agreement with viscosity literature[13,14] and display a steady increase in fragility with increasing addition of Na_2O to the germanium oxide network.

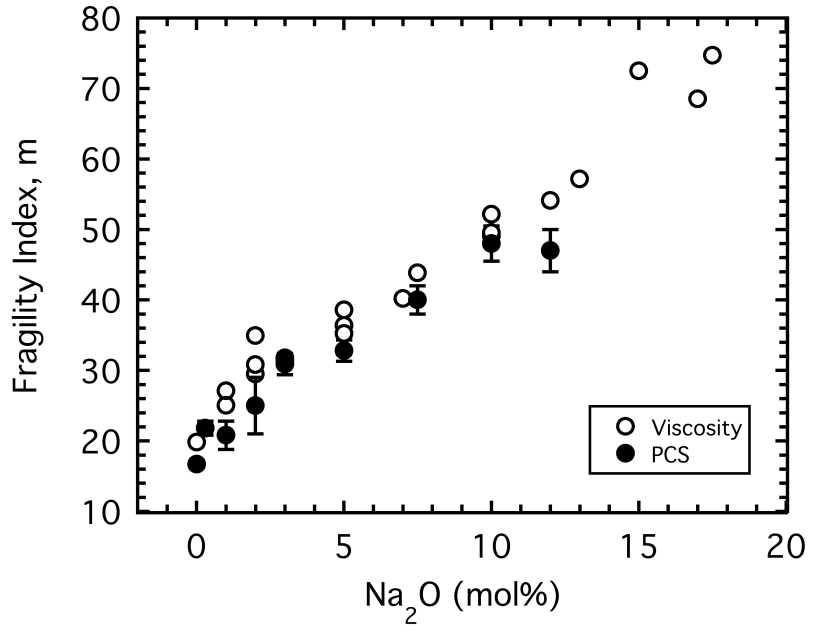

Fig. 4 Compositional dependence of the fragility index determined in present study (PCS) and from viscosity[13,14].

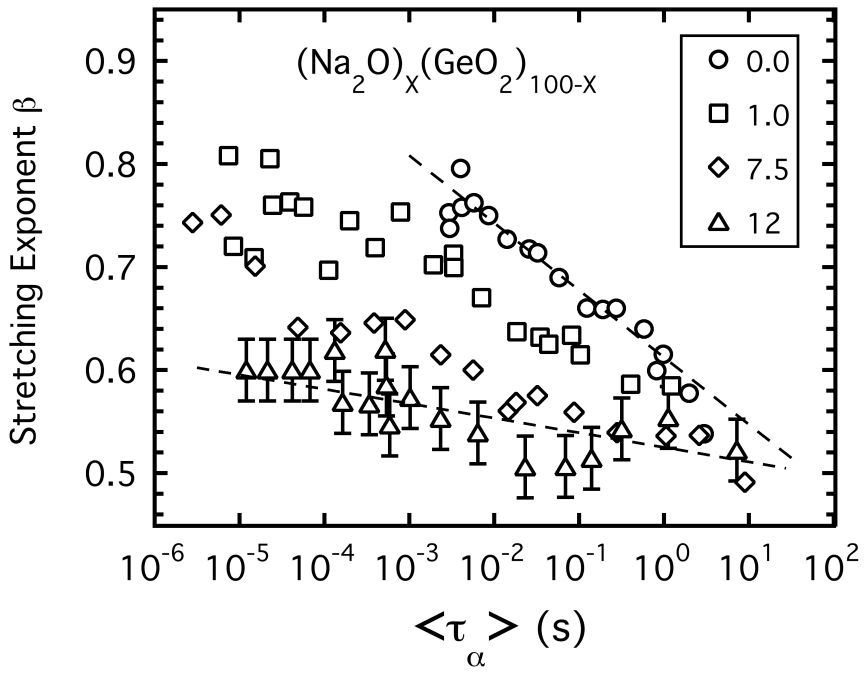

Fig. 5 Plot of the stretching exponent for the α-relaxation as a function of the average relaxation time demonstrating the decrease in β with approach to T_g. Selected compositions shown for clarity. Error bars (± 0.03) shown only for one composition for clarity.

Curve fitting results for the non-exponentiality of the decay are summarized in Fig. 5 where β for selected compositions are plotted together as a function of the $\log_{10}\langle\tau_\alpha\rangle$. Results show that this parameter generally decreases with decreasing temperature as T_g is approached but the rate of decrease, $d\beta/d\log_{10}\langle\tau_\alpha\rangle$, varies continuously with changing sodium content. The slope is steepest for GeO_2 and lowest for x = 12 mol% Na_2O for which the slope is nearly zero. All compositions appear to converge to a value of $\beta(T_g) \approx 0.5$ in the limit that T approaches T_g.

3.3 Slow Ionic Relaxation

The slower relaxation seen in ACFs for concentrations from x = 1 to x = 10 mol% Na_2O was analyzed to determine the temperature dependence of the relaxation time, τ_S, from which the diffusivity of the process can be determined[3] as $D = (\tau_S q^2)^{-1}$ using q = 25.05 μm^{-1}, the scattering wavevector for scattering at 90°. Results are plotted in an Arrhenius fashion as a function of inverse temperature in Fig. 6. Each dataset was fit to an Arrhenius form,

$$D(T) = D_\infty exp\{-E/RT\}, \quad (6)$$

to determine both the amplitude D_∞ and activation energy E. Results provided in Table 1 show that both parameters increase with increasing density of mobile sodium ions.

Table 1: Results of glass transition temperature, fragility and curve fitting for diffusivity.

mol % alkali	$D_\infty(cm^2/s)$	$E\ (kJ/mol)$	T_g (C)	m
0 % Na_2O	-	-	585 (± 5)	16.7 (± 0.3)
0.3 % Na_2O	-	-	487.7 (± 10)	21.8 (± 1)
1 % Na_2O	17.9	190.4	398.7 (± 23)	20.8 (± 2)
2 % Na_2O	1.26 x 10^4	232.0	404.1 (± 25)	25.0 (± 4)

3 % Na_2O	1.77 x 10^5	249.4	431.5 (± 10)	30.9 (± 1.5)
5 % Na_2O	1.97 x 10^5	249.4	441.1 (± 10)	32.8 (± 1.5)
7.5 % Na_2O	8.75 x 10^9	325.9	282.4 (± 10)	40.0 (± 2)
10 % Na_2O	3.2 x 10^{11}	355.8	508.1 (± 10)	48.0 (± 2.5)
12 % Na_2O	-	-	502.8 (± 10)	47.0 (± 3)
5 % K_2O	6.31 x 10^4	252.7	-	-
5 % $(Na/K)_2O$	1.96 x 10^5	251.1	-	-

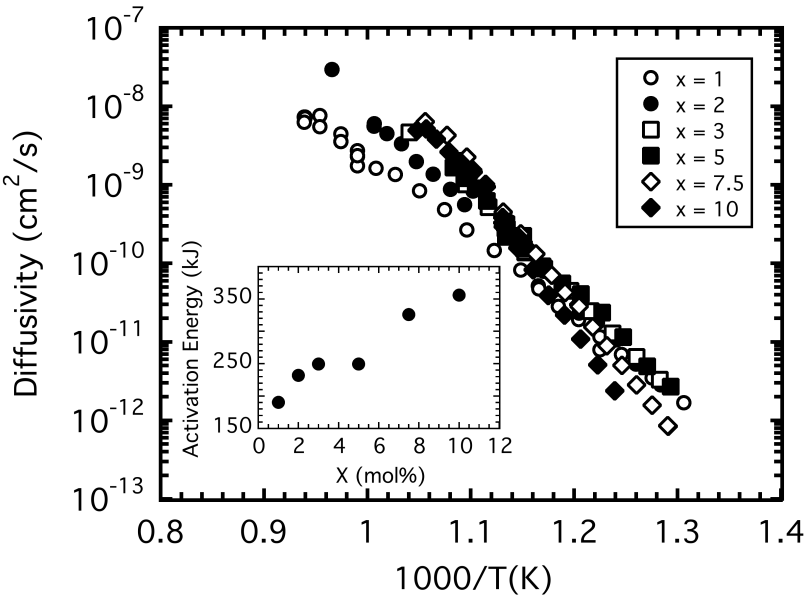

Fig. 6 Diffusivity of the slow relaxation plotted in an Arrhenius manner. Inset shows activation energy determined from fits to Eq. 6.

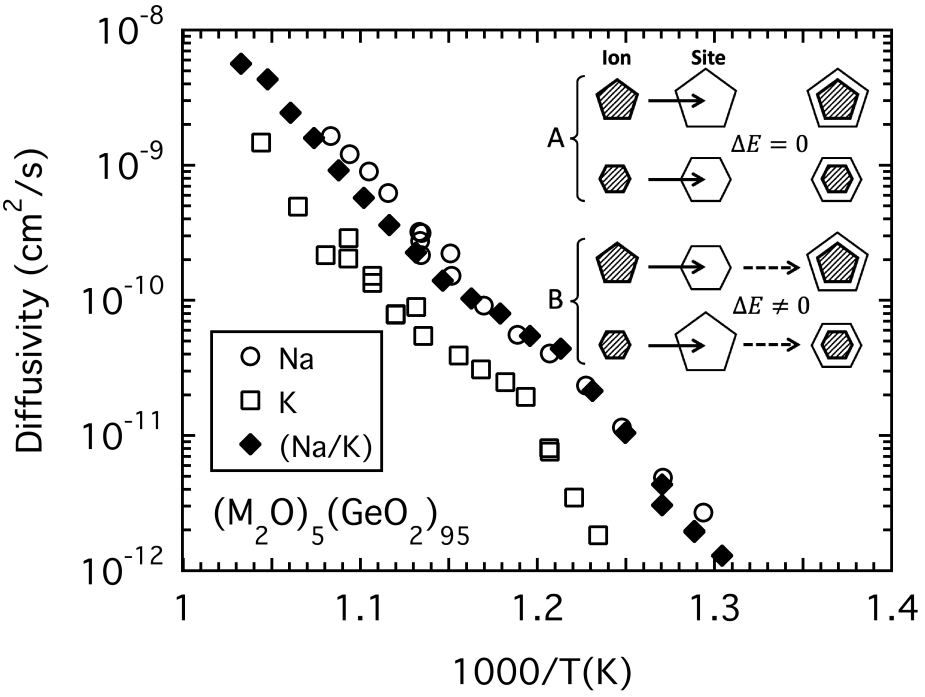

Fig. 7 Diffusivity of the slow relaxation for M = Na, K, and mixed Na/K melts as a function of inverse temperature. Cartoon illustrates the site relaxation model of the mixed alkali effect (discussed in the text): in A, single alkali glasses require no mechanical relaxation for ion hopping. In B, mixed alkali glasses contain ill-configured sites that acquire an energy penalty associated with the need for mechanical relaxation of the network before the ion hopping can proceed.

As an additional study, PCS was conducted also for $(K_2O)_5(GeO_2)_{95}$ and a "mixed alkali" glass melt, $(Na_2O)_{2.5}(K_2O)_{2.5}(GeO_2)_{95}$ to examine how this diffusive process might be influenced by the so-called mixed alkali effect[15,16] which typically results in strong deviations of properties like the conductivity from linear mixing. As shown in Fig. 7, the diffusivity of the potassium germanate melt is mainly displaced to lower values with no substantial change in activation energy while the diffusivity of the mixed alkali melt matches that of the sodium germanate melt.

4. Discussion

4.1 Slow Ionic Relaxation

We begin with the slow, diffusive relaxation process which presents itself almost identically as did a similar slow relaxation in recent study of sodium borate glass melts[11]. In both instances, the slow relaxation was absent at x = 0 mol% Na_2O, increased in amplitude with addition of Na_2O and then vanished again for concentrations above about x = 10 mol%. We have speculated[11] that the slow process represents scattering from concentration fluctuations associated with the movement of the Na ion within the oxide network and that the compositional variation of the amplitude arises from changes in the effective signal-to-noise: at low concentrations, the fluctuations are well distinguished against an otherwise uniform density but as the concentration increases these fluctuations become indiscernible from themselves and the signal-to-noise of the process is lost.

The diffusivity of the slow process appears to be well described by an Arrhenius temperature dependence (see Eq. 6) which is typical for ion diffusion seen in solid glass ion conduction[17,18]. As summarized in Table 1, the diffusivity is characterized by both an amplitude, D_∞, and activation energy E. If the amplitude remained constant, one could then readily associate the activation energy with that thermal energy needed to achieve a given level of diffusivity. However, given the large changes in D_∞ with composition this simple association is less clear. It is also worth commenting that the diffusivity reported here represents the decay of concentration fluctuations which may or may not couple directly with the diffusion of the ions themselves.

More interesting may be the results of the limited mixed alkali studies incorporating Na and K ions. Here we see that at a fixed alkali oxide concentration of x = 5 mol%, D_∞ drops with

no change in activation energy when the Na ion is completely replaced by K (see Fig. 7). This drop is consistent with the expectation that a larger and heavier ion would exhibit a lower diffusivity owing to greater inertia. Curiously, when the Na and K are mixed in equal portions, we see the diffusivity tracks identically with that of the Na only sample, suggesting that the mixing has inhibited the motion of K ions. This finding has some support from current models[16,19] of the mixed alkali effect in ion-conducting solids. These models posit that sites in the oxide network at which an ion resides temporarily before hopping to an adjacent site mechanically relax to accommodate the specific sized ion resulting in two types of site environments; one for each ion species. Ion motion along sites that are similarly configured for a given ion require no further mechanical energy and conduction proceeds well. However, motion is strongly inhibited whenever an ion attempts to enter an ill-configured site - especially a site that must mechanically expand to accommodate the larger cation as would happen when K attempts to enter a Na-configured site. This site mismatch acts to block the motion of the K ion and is likely the reason the diffusivity of the mixed alkali melt mirrors that of the Na only situation.

4.2 The Primary α-relaxation

Like the alkali borate glasses, alkali germanates are renown for exhibiting a compositional "anomaly" in that properties like the glass transition temperature and density exhibit a maximum as a function of added alkali oxide[20]. The explanation for these extremes is that in both systems the addition of alkali oxide does not lead to the formation of non-bridging oxygen (NBO) as occurs in SiO_2, but rather results in increased bridging oxygen (BO) formation that increases the BO bond density. In B_2O_3, the added alkali result in conversion of

3-coordinated (trigonal) B to 4-coordinated (tetrahedral) B while for GeO_2, 4-coordinated Ge is converted to either 5- or 6-coordinated Ge[21,22]. These increases in coordination and BO bond density serve to increase both the mass density and glass transition temperature, respectively. At some point, further addition of alkali oxide begins to generate NBOs that decrease the average coordination and bond density causing both density and T_g to decrease with the result that these properties exhibit an extremum. The extremum is "anomalous" only in the sense that other glass systems like alkali silicates and alkali phosphates only form NBO so that properties like the glass transition decrease rather monotonically.

An unusual feature in sodium germanate system is the appearance of what might be called a "second anomaly" wherein the T_g decreases abruptly (by nearly 200 degrees K) with as little as 1 - 2 mol% added alkali oxide (see Fig. 3) *before* then increasing to a second maximum near 17 mol% associated with the first anomaly described above. This abrupt drop in T_g which is often overlooked is currently not well understood, but may be evidence that some NBO formation does take place with the initial addition of alkali oxide before the onset of increasing BO bond formation[23].

Another interesting observation is the increase in fragility index that occurs as the average BO bond density increases with increasing alkali addition. This trend in fragility is *opposite* that observed in sodium phosphate glass melts whose fragility increased as the bond density decreased. The trend is however similar to that seen in sodium borate glass melts where, despite the increasing BO bond density, the glass fragility increases. In previous work[24,25], we have proposed a possible explanation for these contrary dependences on BO bond density by suggesting that certain rigid structural units (RSUs, such as boroxol rings found

abundantly in B_2O_3) can act to weaken the oxide network against viscous deformations by virtue of redundant BO connections they possess. By coarse-graining over these RSUs we arrived at an adjusted effective bond density for which the fragility of phosphates, borates and many other network forming glasses collapse to a common dependency on network bond connectivity[26]. This includes the alkali germanates where, according to recent Raman studies[27], small rings are present in GeO_2 (much like those in B_2O_3) which rapidly grow in number between x = 0 to x = 10 mol%. By modeling[28] this ring growth and making statistical assumptions as to the fractions of possible ring-to-ring connections, we could again arrive at a coarse grained connectivity that places the fragility of alkali germanates onto the above mentioned master curve.

Lastly, we consider trends in the non-exponentiality of the α-relaxation with changes in the BO bond density of the alkali germanate network. In Fig. 5 we see that for GeO_2 the stretching exponent decreases steadily with approach to T_g (where $\log_{10}\langle\tau_\alpha\rangle$ = 2). A similar decrease of β approaching T_g was seen in all other alkali germanate melts, but the slope of decrease became smaller with increasing alkali oxide. A similar pattern was observed in sodium phosphate glass melts with zero slope observed just near the average BO bond density, $\langle n\rangle$ = 2.4. This particular bond density has special relevance in constraint counting models of bonded networks as it represents a *rigidity percolation* transition[29,30] where the number of mechanical constraints imposed by added bonds just begins to exceed the degrees of freedom of the objects being bonded. In this instance of oxide glasses, it is the degrees of freedom of the tetrahedral-octahedral objects which are just being balanced by an equal number of constraints due to BO connections between. The transition is often described[30] as one of

"floppy" network structures that are under constrained becoming "rigid" and over constrained and marks a significant mean field benchmark in the evolution of the network with composition. It is interesting then that near this special average bond density we find $\beta(T)$ approximately constant indicating that the shape of the decay process becomes independent of temperature and exhibits *thermorheological simplicity* (TRS) in that each spectrum could be rescaled in time to collapse onto a common decay.

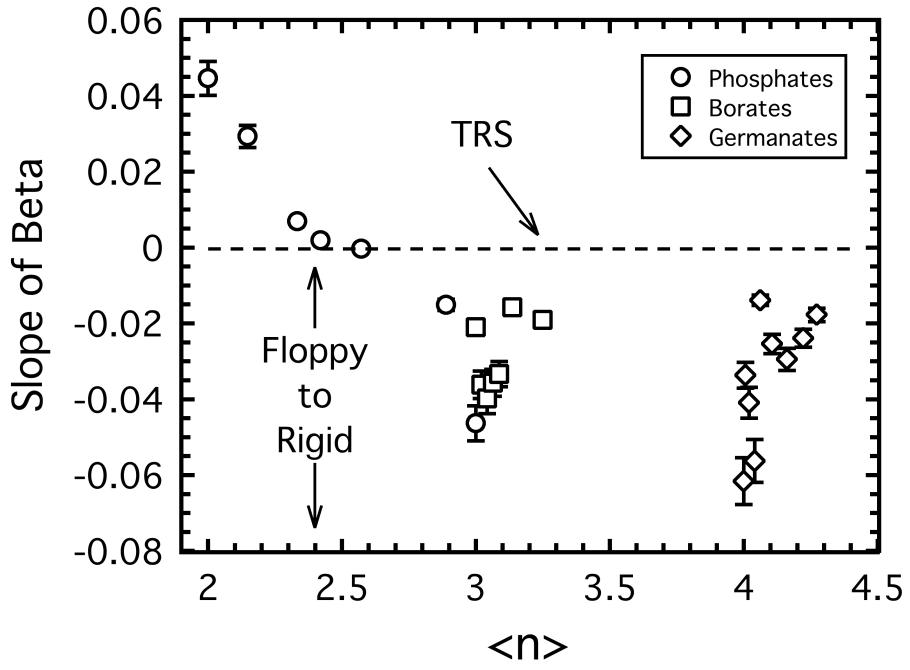

Fig. 8 Slope of stretching exponent defined in text as a function of average bridging oxygen bond density for sodium phosphates[9], borates[11] and germanates. Dashed line indicates zero slope where thermorheological simplicity applies and vertical arrow locates the rigidity percolation point at $\langle n \rangle$ = 2.4.

In Fig. 8 we have plotted the slope ($d\beta/d\log_{10}\langle\tau_\alpha\rangle$) of the stretching exponent as a function of the average BO bond density, $\langle n \rangle$, in three alkali oxide systems we have now studied. Unlike the alkali phosphate which shows a strong trend with $\langle n \rangle$, neither the borate nor the germanates appear to show any strong dependence on $\langle n \rangle$ although each exhibit negative slope at large $\langle n \rangle$ that is consistent with the trend set by the phosphate data set. Only the phosphate

data set include positive slopes seen at $\langle n \rangle < 2.4$ as the network structure evolves toward polymeric chains of linked tetrahedra.

In Fig. 5 we had highlighted the apparent convergence of $\beta(\log_{10}\langle\tau_\alpha\rangle)$ to values of $\beta(T_g) \approx 0.5$ as T_g is approached (where, by definition $\log_{10}\langle\tau_\alpha\rangle = 2$). This convergence has been seen in both borates and phosphates despite the broad range of network forming structures that span 2d polymeric to highly bonded 3d continuous networks and include melts with fragilities from m = 80 to 17, respectively. In Fig. 9 we have collected these values of $\beta(T_g)$

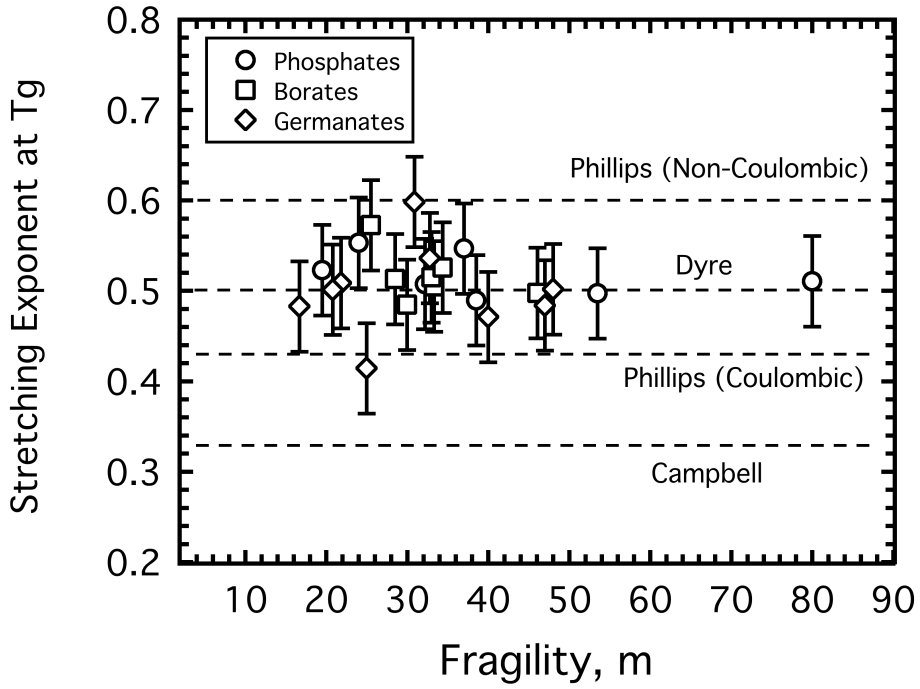

Fig. 9 Limiting value of the stretching exponent at T_g plotted against the fragility index for sodium phosphate[9], borate[11] and germanate melts. Horizontal dashed lines highlight special values of $\beta(T_g)$ proposed by models[31-34] in the literature.

obtained by a short extrapolation to $\log_{10}\langle\tau_\alpha\rangle = 2$ for all three network forming oxides that we have now studied as a function of their fragility index. Included in the figure are horizontal lines that mark a handful of special values for $\beta(T_g)$ that have been expressed in relaxation models

over the years. In the early work of Campbell[31] the authors considered a model of diffusion in a percolating phase space to predict that near T_g, relaxations would become increasingly stretched with $\beta(T_g)$ = 1/3. In a later model by Phillips[32], the diffusion between randomly placed traps served as a model of relaxation with two special stretching exponents; $\beta(T_g)$ = 3/5 for non-Coulombic interactions and $\beta(T_g)$ = 3/7 for Coulombic interactions. Far more recently, Dyre[33] has re-examined a large volume of dielectric relaxation measurements to argue that many appear to exhibit a universal value of $\beta(T_g)$ = 1/2 which can be easily explained by several simple relaxation models[34].

In Fig. 9, we see our collected results for network forming oxides span in between the two values of $\beta(T_g)$ proposed by Phillips[32] and are clearly too large for the $\beta(T_g)$ = 1/3 prediction by Campbell[31]. In fact, the findings are more consistent with the proposal by Dyre[34] that there may be a universal value, seen in both molecular liquids and network forming oxides, of $\beta(T_g)$ = 1/2.

It is also worth noting that the pattern in Fig. 9 does not suggest any correlation of $\beta(T_g)$ with fragility within this sample of oxide melts. This is at odds with earlier surveys[4], conducted with both network forming oxides, molecular liquids and organic polymers that had concluded $\beta(T_g)$ generally increases with decreasing fragility.

5. Conclusions

Numerous studies on molecular liquids and organic polymers have demonstrated that the primary α-relaxation in these materials decays in a non-exponential manner with a timescale that is non-Arrhenius in temperature. These features appear to be hallmarks of the

highly cooperative molecular rearrangements happening in highly viscous super cooled liquids just near the glass transition. But far fewer studies have probed these same viscous dynamics in network forming oxide melts where one anticipates that variations in the bonding structure of the network would likely influence the character of the dynamics.

Our current study of sodium germanate melts not only adds to a growing list of network forming oxides studied using PCS, but when viewed alongside previous studies of sodium borates and phosphates, begins to establish some concurrent trends in the nature of the relaxation. For example, the glass transition temperature appears to increase with increasing BO bond density for all three oxide systems supporting the idea that in these over constrained networks it is bond scission-renewal required to initiate molecular-level rearrangements. As for the fragility, there is a general trend that it increases with increasing addition of alkali oxide. However, the structural changes in network bond density due to increasing alkali oxide are not alike for these systems: in phosphates, the BO bond density decreases with alkali oxide but in both the borates and germanates it increases. Hence, when fragility is viewed with regards to changes in the average bond density of the oxide network, there is no consistent pattern unless one adopts a modified definition of network connectivity that incorporates coarse-graining over certain rigid structural units[26].

Finally, we can conclude that for over constrained networks with average BO bond density of $\langle n \rangle > 2.4$ the stretching exponent generally decreases with decrease in temperature on approach to T_g, while for some under constrained sodium phosphate networks with $\langle n \rangle < 2.4$ the exponent increases with decreasing temperature. Even more consistent is the tendency for

this exponent to approach a universal value of $\beta(T_g)$ = 1/2 in the limit that T_g is approached independent of both fragility and BO bond density considerations.

Acknowledgement: This material is based upon work supported by the National Science Foundation under Grant No. (DMR-2051396)

References

**. Y. Luo, C. Qu, A. Bhadu , J. C. Mauro, Synthesis and characterization of K_2O-ZnO-GeO_2-SiO_2 optical glasses, J. Non-Cryst. Sol. 503-504 (2019) 308 - 312.

1. P.G. Debenedetti, F.H. Stillinger, Supercooled liquids and the glass transition, *Nature* **410** (2001) 259 - 267.

2. M.D. Ediger, C.A. Angell, S.R. Nagel, Supercooled liquids and glasses, *J. Phys. Chem.* **100** (1996) 13200-13212.

3. Berne, B. J. and Pecora, R. *Dynamic Light Scattering* (John Wiley & Sons, New York, 1976).

4. R. Boehmer, K.L. Ngai, C.A. Angell, D.J. Plazek, Nonexponential relaxations in strong and fragile glass formers*, J. Chem. Phys.* **99**(5) (1993) 4201 - 4209.

5. A. I. Nielsen, T. Christensen, B. Jakobsen, K. Niss, N. B. Olsen, R. Richert, J. C. Dyre, Prevalence of approximate $\sqrt{t}$ relaxation for the dielectric α process in viscous organic liquids, *J. Chem. Phys.* **130**, 154508 (2009).

6. F. Pabst, J. P. Gabriel, T. Boehmer, P. Weigl, A. Helbling, T. Richter, P. Zourchang, T. Walther, and T. Blochowicz, Generic structural relaxation in supercooled liquids, *J. Phys. Chem. Lett.* **12**:3685 - 3690 (2021).

7. D. Sidebottom, R. Bergman, L. Borjesson and L. M. Torell, Two-step relaxation decay in a strong glass former, *Phys. Rev. Lett.* **71**:2260-2263 (1993).

8. D. L. Sidebottom, B. V. Rodenburg and J. R. Changstrom, "Connecting Structure and Dynamics in Glass Forming Materials by Photon Correlation Spectroscopy," *Phys. Rev. B* **75**, 132201 (2007).

9. R. Fabian, Jr., D.L. Sidebottom, Dynamic light scattering in network-forming sodium ultra-phosphate liquids near the glass transition, *Phys. Rev. B* **80** (2009) 064201.

10. Tri D. Tran and D. L. Sidebottom, “Glass-forming Dynamics of Aluminophosphate Melts Studied by Photon Correlation Spectroscopy,” *J. Am. Ceram. Soc.* **96**, 2147 (2013).

11. H. Uppala and D. L. Sidebottom, “Evidence for ionic diffusion in dynamic light scattering from glass-forming sodium borate melts" *J. Non-Cryst. Sol.* **588***,* 121627 (2022).

12. D. L. Sidebottom, “Generic α-relaxation in a strong GeO2 glass melt" *Phys. Rev. E* **107***,* L012602 (2023).

13. S. V. Nemilov, Systematic study of the influence of admixtures of sodium oxide on the viscosity of glassy germanium dioxide, *Zh. Prikl. Khim*. **45**:256 - 262 (1972).

14. J. E. Shelby, Viscosity and thermal expansion of alkali germanate glasses, *J. Am. Ceram. Soc.* **57**(10): 436 -439 (1974).

15. J. O. Isard, The mixed alkali effect in glass*. J. Non-Cryst. Sol.* **1**(3): 235-261 (1969).

16. M. D. Ingram and B. Roling, The concept of matrix-mediated coupling: a new interpretation of mixed-cation effects in glass. *J. Phys.: Cond. Matt.* **15**(16): S1596 (2003).

17. J. C. Dyre, P. Maass, B. Roling and D. L. Sidebottom, Fundamental questions relating to ion conduction in disordered solids. *Rep. Prog. Phys.* **72**(4): 046501 (2009).

18. D. L. Sidebottom, “Evidence for Site Memory Effects in the Ionic Relaxation of $(Li_20)_x(Na_20)_y(GeO_2)_{1-x-y}$ Glasses,” *J. Non-Cryst. Solids* **255**, 67 (1999).

19. J. Swenson and S. Adams, Mixed alkali effect in glasses. *Phys. Rev. Lett.* **90**(15): 155507 (2003).

20. J. E. Shelby, Thermal expansion of alkali borate glasses. *J. Am. Ceram. Soc.* **66**(3): 225-227 (1983).

21. D. L. Griscom, Borate Glass: Structure, Properties and Applications, in L. D. Pye, V. D. Frechette and N. J. Kreidl (Eds), Plenum Press, New York 1978, pp. 11-149.

22. A. Hannon, D. Di Martino, L. F. Santos and R. M. Almeida, A model for the Ge-O coordination in germanate glasses. *J. Non-Cryst. Sol.* **353**: 1688-1694 (2007).

23. to be published

24. D.L. Sidebottom, S.E. Schnell, Role of intermediate-range order in predicting the fragility of network-forming liquids near the rigidity transition, *Phys. Rev. B* **87** (2013) 054202.

25. D. L. Sidebottom, “Connecting glass-forming fragility to network topology." *Frontiers in Materials* **6,** 114 (2019).

26. D.L. Sidebottom, Fragility of network-forming glasses: A universal dependence on the topological connectivity. *Phys. Rev. E* **92** (2015) 062804.

27. G. S. Henderson, The germanate anomaly: What do we know*? J. Non-Cryst. Sol*. **353**: 1695-1704 (2007).

28. D. L. Sidebottom, T. D. Tran and S. E. Schnell, “Building up a weaker network: The effect of intermediate range glass structure on liquid fragility,” *J. Non-Cryst. Solids* **402**, 16 (2014).

29. J.C. Phillips, Topology of covalent non-crystalline solids I: Short-range order in chalcogenide alloys. *J. Non-Cryst. Sol.* **34**(2): 153-181 (1979).

30. H. He and M. F. Thorpe, Elastic properties of glasses. Phys. Rev. Lett. **54**(19): 2107-2110 (1985).

31. I. A. Campbell, J. M. Flesselles, R. Jullien ad R. Botet, Nonexponential relaxation in spin glasses and glassy systems. *Phys. Rev. B* **37**(7) 3825 - 3828.

32. J.C. Phillips, Stretched exponential relaxation in molecular and electronic glasses. *Rep. Prog. Phys.* **59**: 1133 (1996).

33. J.C. Dyre, Colloquium: The glass transition and elastic models of glass-forming liquids, *Rev. Mod. Phys.* **78** (2006) 953 - 972.

34. J. C. Dyre, A model for the generic alpha relaxation of viscous liquids, *Europhys. Lett.* **71**, 646 (2005).